Національна академія наук України

ІНСТИТУТ
ФІЗИКИ
КОНДЕНСОВАНИХ
СИСТЕМ

ICMP–98–33E

Ja. M. Ilnytskyi, S. Sokołowski,* O. Pizio†

**ON THE NEMATIC-ISOTROPIC TRANSITION IN A LATTICE MODEL WITH QUENCHED DISORDERED IMPURITIES. A MONTE CARLO STUDY.**

*Department for the Modelling of Physico-Chemical Processes, Faculty of Chemistry, MSC University, 200-31 Lublin, Poland

†Instituto de Quimica de la UNAM, Coyoacan 04510, Mexico, D.F.

ЛЬВІВ

**УДК:** 532.783:548-14; 536.425

**PACS:** 61.30.Cz, 64.60.Cn, 02.70.Lq

**Фазовий перехід нематик-ізотропна рідина в гратковій моделі з замороженими домішками. Комп'ютерна симуляція за допомогою методу Монте Карло**

Я. М. Ільницький, С. Соколовскі, О. Пізіо

**Анотація.** Виконано Монте Карло симуляції граткової моделі, яка описує поведінку рідкого кристалу при наявності заморожених домішок. На відміну від випадку чистої системи, у якій відбувається достатньо сильний орієнтаційний перехід першого роду, при наявності 5% домішок цей перехід є суттєво слабшим. Досліджується зсув температури переходу, пониження теплоти переходу, параметру впорядкування, теплоємності та сприйнятливості, що викликано наявністю домішок. Використовується гістограмна техніка та аналіз числових даних за допомогою скінченновимірного скейлінгу. Виконано порівняння із експериментами над рідкими кристалами в аерогелях та пористих склах.

**On the nematic-isotropic transition in a lattice model with quenched disordered impurities. A Monte Carlo study.**

Ja. M. Ilnytskyi, S. Sokołowski, O. Pizio

**Abstract.** We have performed Monte Carlo (MC) simulations of the lattice model mimicking liquid crystalline behavior in the presence of disordered quenched impurities. A well pronounced first order nematic-isotropic transition has been obtained for a bulk pure model. However, at a 5% concentration of impurities, we have observed a very weak first order transition being suppreseed as compared to a pure case. We have discussed a shift of the transition temperature, a suppression of the latent heat and the maxima of the heat capacity and susceptibility due to the presence of impurities. A histogram analysis and a finite-size scaling has been applied to the MC data. A comparison of the simulation data with the experimental results for liquid crystals confined to silica aerogels and porous glasses also has been performed.

**Подається в** Physical Review E
**Submitted to** Physical Review E

© Інститут фізики конденсованих систем 1998
Institute for Condensed Matter Physics 1998

## 1. Introduction

The structure, thermodynamics and phase behavior of fluids confined to disordered porous media has received much attention during last decade. A large amount of the experimental, simulational and theoretical results have been accumulated. On the other hand, more interesting, and physically richer, complex fluids under confinement have received less attention. The liquid crystalline materials in confined geometry are of particular interest for basic science and for applied research.

Interest to liquid crystals (LCs) in the individual pores and in disordered porous media is very rapidly increasing, see, e.g. [1–16]. In particular, the nematic-isotropic (NI) transition in liquid crystals confined to microporous and mesoporous media has been studied experimentally [5–9]. The experimental results provide evidence that the finite size of pores, the effect of quenched disorder and the interconnectivity of pores, are main factors that influence phase behaviour of LCs in microporous adsorbents. Theoretical investigation and simulation of the NI transition in porous media therefore must include modelling of the various factors crucial to the NI transition [10–16].

A set of numerical studies of liquid crystalline materials in microporous media has been attempted during last decade. In particular, a model of trimers on a simple cubic (sc) lattice has been simulated by Dadmun and Muthukumar [12]. A porous medium has been implied as a dilution, i.e. it has been assumed that a fraction of sites of the lattice is unaccessible for trimers. The excluded volume effects of dilution have yielded lower temperature of the NI transition temperature and rounder heat capacity maximum of the model, if compared to its pure counterpart. Moreover, the transition has been shown to change its nature from the first to the second order, if the concentration of impurities is larger than 2.5%. The simulation data have been shown to agree qualitatively with the experimental results. However, quantitatively the shift of the transition temperature compared to the pure model, i.e. in the absence of impurities, is essentially overestimated. It seems that, the size of the lattice system considered in Ref. [12] (up to 16x16x16 sites, such that the system consists of less than 1300 trimers) is insufficient to describe the thermodynamics quantitatively.

A study of the phase transitions in aerogel has been undertaken by Uzelac *et al.* [13] in the framework of the $q = 3$ and $q = 4$ Potts models. The models are characterized by a weak first order transition in the pure case. The aerogel has been modelled as a set of correlated impurities on the lattice by using diffusion-limited cluster-cluster aggregation; the case



of randomly distributed impurities also has been studied in [13]. A finite size scaling analysis (on the lattices up to $20^3$ size) and the Ferrenberg-Swendsen (FS) histogram technique [17] have been used. The shift of the transition temperature with increasing concentration of impurities appeared to be smaller in the aerogel case, comparing with the case of randomly distributed impurities. The heat capacity peaks have been obtained as suppressed and essentially broadened with increasing impurity concentration. The finite-size scaling analysis of the simulation data has shown that the order of the transition for 3D $q = 3$ and $q = 4$ Potts models changes at a nonzero concentration threshold. However, these results must be considered with some care due to small lattice sizes involved, and due to the fact that systematic averages over disorder have not been performed. Neverhteless, the results presented in Ref. [13] confirm that even a weak dilution may essentially affect the NI transition (these trends were observed earlier by Hashim *et al.* [18]).

Other models and theoretical developments concerning the behavior of liquid crystalline materials in the presence of the quenched disorder have been proposed recently, particularly, random-field Ising model [10, 11], random anisotropy nematic model [15], single-pore model for liquid crystal in aerogel [16].

In general, computer simulations are powerful tools to investigate a microscopic nature of the liquid crystalline phases. The most successfull intermolecular potentials applied in the simulations of the bulk models include the Berne-Pechukas [19] and Gay-Berne [20] potentials. However, reasonably large systems of molecules interacting via these potentials, appropriate to study phase transitions, are difficult to consider due to computer time consumption. Therefore, for practical reasons, it is important to obtain the simulation results for large systems of molecules in the framework of quite simple models, intrinsically preserving liquid crystalline nature.

With this aim, in the present study we perform Monte Carlo simulations of the NI transition in a modified Lebwohl-Lasher (LL) lattice model for liquid crystals [21], however, both in its pure state and in the presence of quenched random dilution. The particles in the model interact via the angular part of the Berne-Pechukas (BP) potential [19] derived from the overlap integral of two ellipsoidal Gaussians of a certain elongation $a$. The first order NI transition in the pure modified LL model becomes stronger with increasing elongation parameter [21]. We consider the case $a = 3$, that yields reasonable values for the latent heat and for the order parameter at the NI transition [21]. Our investigation of the model in the presence of a microporous media, is restricted to the case of

a 5% dilution (which formally corresponds to a highly porous medium). A more "liquid crystalline" model is used in the present study, in comparison with previous works [12,13]. Consequently, the simulations are much more time consuming. Moreover, the lattice sizes up to $24^3$ are simulated and a wide set of thermodynamical properties is discussed close to the NI transition. We would like to investigate how the dilution affects thermodynamic properties near the NI transition, and if the transition remains of the first order. On the other hand, our intention is to perform comparison with the available experimental results on LCs in highly porous confining media. A finite-size scaling analysis and the FS histogram technique [17] are used in the analysis of the simulation results.

## 2. The Nematic-Isotropic Transition in the Pure Model

We consider a lattice model of elongated particles interacting via an angular part of the BP potential. The last one has a following form [19]:

$$V_{BP}(\hat{u}_i, \hat{u}_j, \vec{r}) = 4\,\epsilon(\hat{u}_i, \hat{u}_j) \cdot \left[ \left( \frac{\sigma(\hat{u}_i, \hat{u}_j, \hat{r})}{r} \right)^{12} - \left( \frac{\sigma(\hat{u}_i, \hat{u}_j, \hat{r})}{r} \right)^{6} \right],$$

where $\epsilon(\hat{u}_i, \hat{u}_j)$ and $\sigma(\hat{u}_i, \hat{u}_j, \hat{r})$ are the effective orientationally dependent strength and range parameters, respectively. The unit vectors $\hat{u}_i, \hat{u}_j$ are directed along the corresponding long axes of the interacting $i, j$-th ellipsoids, $\vec{r}$ is the center-of-mass distance vector between them, and $\hat{r}$ is the unit vector along $\vec{r}$. In the case of rotators $\hat{u}_i$ on a lattice with the nearest neighbors interaction only the angular dependence of $\epsilon(\hat{u}_i, \hat{u}_j)$

$$\epsilon(\hat{u}_i, \hat{u}_j) = \frac{\epsilon_0}{\sqrt{1 - \chi^2 \cos^2 \theta_{ij}}} \tag{1}$$

is involved ($\theta_{ij}$ is the angle between $\hat{u}_i$ and $\hat{u}_j$). The anisotropy of ellipsoids is characterized by the anisotropy parameter:

$$\chi = \frac{a^2 - 1}{a^2 + 1}, \qquad a = \frac{\sigma_\parallel}{\sigma_\perp},$$

where $\sigma_\parallel, \sigma_\perp$ are their major and minor axes, and $a$ denotes the elongation parameter. In our computer simulations we use the following normalized interparticle interaction,



$$V_{BPA}(\theta_{ij}) = -\frac{\epsilon}{2} \left[ \frac{6a}{(a-1)^2} \left( \frac{1}{\sqrt{1 - \chi^2 \cos^2 \theta_{ij}}} - 1 \right) - 1 \right], \tag{2}$$

where

$$\epsilon = \frac{(a-1)^2}{3a} \epsilon_0 \tag{3}$$

is the parameter used as energy unit in our simulations. For the sake of convenience, this potential is normalized such that at $\theta_{ij} = 0$ and at $\theta_{ij} = \frac{\pi}{2}$ it gives the same energy (in units of $\epsilon$) as the LL potential [22]. Moreover, the LL potential is reproduced in the limit of small anisotropy ($\chi \ll 1$) by expanding the expression given by Eq. 2 in powers of $\chi$:

$$\lim_{\chi \ll 1} V_{BPA}(\theta_{ij}) = -\epsilon P_2(\cos \theta_{ij}) + \text{const.}$$

The first order NI transition, that has been observed in the model at hand, becomes stronger with the increasing elongation parameter $a$ [21]. However, the parameter $a$ provides only a rough estimate of the elongation of real molecules; more reasonable is just to think that the anisotropy of the intermolecular potential increases with augmenting value of the parameter $a$. On the other hand, stronger anisotropy can be achieved by adding higher $P_{2n}$ terms to the LL potential [23–25] and choosing the expansion coefficients appropriately.

We restrict ourselves to the case $a = 3$ in Eq. 2 (it is interesting to mention that in this case $V_{BPA}(\theta_{ij})$ coincides well with the potential considered by Romano [26] expanded up to $P_6$ term). The value $a = 3$ also has been used in the simulations of the Gay-Berne model [20].

We have performed simulations of the pure model with the potential $V_{BPA}(\theta_{ij})$ for four different lattice sizes $16^3$, $18^3$, $20^3$, $24^3$ and apply a finite-size scaling analysis and the FS reweighting technique for the data obtained. Our principal interest is in the properties that are expected to change at a weak dilution. These are the transition temperature, the maximum values for the specific heat and susceptibility, the minima for the fourth Binder's cumulant, the latent heat and the order parameter at transition.

A numerical procedure for each lattice size was similar. First, short scanning runs (up to $10^5$ MC cycles) were performed for the entire interval of temperatures including the NI transition point. Then we select a temperature for which a number of configurations (along the run), with predominant nematic or isotropic phase, is of the same order. A good indication for that is a regular "flow" of the order parameter values from

about 0.05 to 0.3. At such a temperature, we would say, the coexistence of two phases is observed. Then, an extended run of the $5 \cdot 10^5$ MC cycles was performed at this temperature and the histograms of energy and of the order parameter have been built up. By applying the FS reweighting the NI transition point was located in the first approximation. This estimate for the NI transition temperature is used for the final extended run of not less than $10^6$ MC cycles that provides final histograms and the quantities of interest.

A standard Metropolis algorithm has been used in our simulations. The orientation of each particle $\hat{u}_i$ was attempted to change by adding a vector $\vec{l}$ with random orientation and of controlled length [27], and then normalizing the value $\hat{u}_i^{'} = \hat{u}_i + \vec{l}$ back to unity. A new configuration was accepted, if the energy becomes lower, or accepted with a Boltzmann probability otherwise. The length of $\vec{l}$ has been adjusted during simulation to provide a ratio of accepted attempts approximately equal to 0.4. The dimensionless temperature $T^* = k_B T/\epsilon$ is used in the simulations.

Each configuration is characterized by the one-particle energy

$$U^* = \frac{1}{N_f\,\epsilon} \sum_{ij} V_{BPA}(\theta_{ij})$$

($N_f$ is the number of unit vectors $\hat{u}_i$ in the simulation box) and the order parameter,

$$S = \langle P_2(\cos\vartheta_i)\rangle_i,$$

where $\theta_i$ is the angle between $\hat{u}_i$ and a director. The order parameter is calculated after each simulation cycle as the largest eigenvalue of the corresponding tensor [28].

The values of $U^*$ and $S$ have been stored after each MC cycle along the extended run at temperature $T_0^*$. These arrays were used to build up the normalized histograms of energy $P_{T_0^*}(U^*)$ and of the order parameter $P'_{T_0^*}(S)$ distribution at $T_0^*$; these distributions can be presented in the form (slight modification of the formulae of Ferrenberg and Swendsen [17] is used):

$$\begin{aligned} P_{T_0^*}(U^*) &= \frac{1}{Z_0} w(U^*) \exp(-\frac{E(U^*)}{k_B T_0}), \\ P'_{T_0^*}(S) &= \frac{1}{Z'_0} w'(S) \exp(-\frac{E'(S)}{k_B T_0}), \end{aligned} \tag{4}$$

where $w^{(')}(M)$ is the number of states with the corresponding value of $M$, and $E^{(\prime)}(M)$ is the energy of that state. The factor $Z_0^{(\prime)}$ has been



introduced for the sake of normalization. Evidently, the function $E(U^*)$ is simply $N_f\,\epsilon\,U^*$ and, correspondingly, $E'(S) = N_f\,\epsilon\,U^*(S)$, where $U^*(S)$ is the histogram for the energy distribution versus given values of the order parameter $S$. As a result, we can rewrite Eqs. 4 in the form:

$$\begin{aligned} P_{T_0^*}(U^*) &= \frac{1}{Z_0} w(U^*) \exp(-\frac{U^* N_f}{T_0^*}), \\ P'_{T_0^*}(S) &= \frac{1}{Z'_0} w'(S) \exp(-\frac{U^*(S) N_f}{T_0^*}). \end{aligned} \tag{5}$$

As far as $w^{(')}(M)$ are temperature independent the corresponding distributions at some nearby temperature $T^*$ can be derived analytically by simple reweighting of the expressions given by Eq. 5 [17]:

$$\begin{aligned} P_{T^*}(U^*) &= \frac{1}{Z} P_{T_0^*}(U^*) \exp(-(\frac{1}{T^*} - \frac{1}{T_0^*}) U^* N_f), \\ P'_{T^*}(S) &= \frac{1}{Z'} P'_{T_0^*}(S) \exp(-(\frac{1}{T^*} - \frac{1}{T_0^*}) U^*(S) N_f), \end{aligned}$$

where $Z^{(\prime)}$ serves as a new normalization constant at $T^*$. These distributions are used then to calculate the average momenta of $U^*$ and $S$ at $T^*$:

$$\langle U^{*n}\rangle = \sum_i U_i^{*n}\, P_{T^*}(U_i^*), \qquad \langle S^n\rangle = \sum_i S_i^n\, P'_{T^*}(S_i),$$

from which we obtain a set of quantities of interest. Particularly, the dimensionless heat capacity, $C_v^* = C_v/(k_B N_f)$, and the susceptibility, $\chi^* = \chi\epsilon/N_f$, can be defined via the fluctuational formulae:

$$C_v^* = \frac{N_f}{T^{*2}}(\langle U^{*2}\rangle - \langle U^*\rangle^2), \qquad \chi^* = \frac{N_f}{T^*}(\langle S^2\rangle - \langle S\rangle^2)$$

Also, we have calculated the fourth Binder's cumulant of the energy fluctuations [29] as follows:

$$V_4 = 1 - \frac{\langle U^{*4}\rangle}{3\,\langle U^{*2}\rangle^2},$$

which is a useful additional estimate of the transition temperature, and serves to determine the order of the transition.

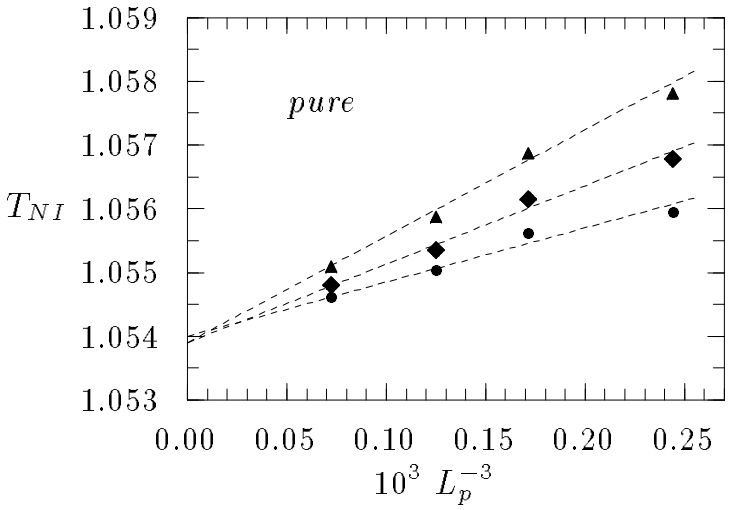


Figure 1. Finite-size scaling behavior of the NI transition temperature in the pure model defined by different ways (circles and diamonds are obtained from the peaks of the heat capacity and the susceptibility, respectively, triangles are from the minima of the fourth Binder's cumulant), $L_p$ is the linear size of the simulated model.

Let us denote the NI transition temperature (estimated in the framework of a procedure numbered by $m$) by $T^*_{m,NI}(L_p)$ for the system of $L_p^3$ size, $p$ is the subscript introduced to emphasize the pure case. For the first order transition, we would expect from Ref. [30], that $T^*_{m,NI}(L_p) - T^*_{m,NI}(\infty_p) \sim L_p^{-3}$, where $T^*_{m,NI}(\infty_p)$ is the transition temperature for an infinite system. Following Ref. [31] we have used three different procedures to evaluate the NI transition temperature for each system size. The locations of the peaks for $C^*_v(L_p)$ and $\chi^*(L_p)$ yield $T^*_{1,NI}(L_p)$ and $T^*_{2,NI}(L_p)$ respectively, and a location of the $V_4$ minimum gives $T^*_{3,NI}(L_p)$. The expected finite-size scaling behaviour holds exactly for all $T^*_{m,NI}(L_p)$ (see, Fig. 1); this behavior is quite similar to the one observed for the LL model [31]. The fitting lines meet at $L = 0$, giving the value

$$T^*_{NI}(\infty_p) = 1.0540 \pm 0.0002 \qquad (6)$$

for an infinite system. We must mention that this value cannot be compared straightforwardly with the one for the LL model [31] due to a different energy scale ($\epsilon$ given by Eq. 3 is anisotropy dependent).



Another common test for the first order transition is the scaling of the maxima for $C^*_{v\,\max}(L_p)$ and for $\chi^*_{\max}(L_p)$ proportionally to $L_p^3$, with increasing $L_p$. We have obtained typical rounded peaks for $C^*_v(L_p)$ and $\chi^*(L_p)$; both become higher, narrower and shift to a lower value of $T^*$ as $L_p$ increases. For the sake of brevity, we do not present these curves in the present work (see, e.g. Refs. [13,31,32]). The values for $C_{v\,\max}(L_p)$ and for $\chi_{\max}(L_p)$ versus $L_p^3$, together with the corresponding fitting lines are shown in Fig. 2. One can see that the scaling law of the $L_p^3$ type is satisfied very well.

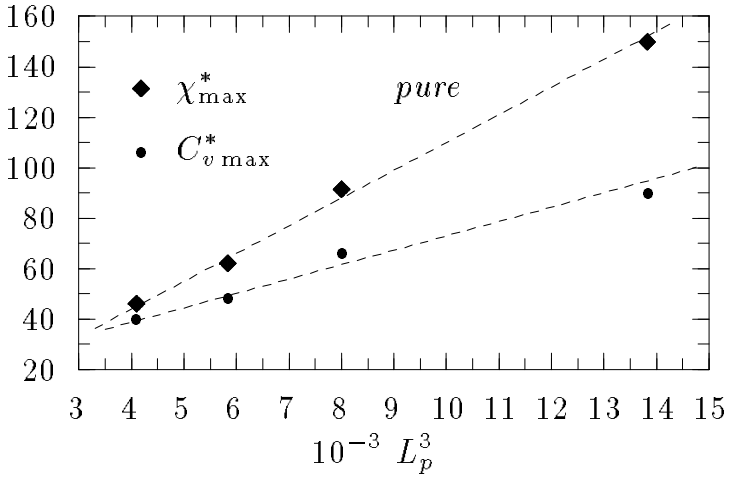


Figure 2. Finite-size scaling behavior of the heat capacity, $C^*_{v\,\max}$, and the susceptibility, $\chi^*_{\max}$, maxima in the vicinity of the NI transition in the pure model of linear size $L_p$.

The properties that can be compared with the experiment are the latent heat at the NI transition $\Delta H_{NI}(L_p)$ and the order parameter $S_{NI}(L_p)$ at $T_{NI}$. To obtain the value for $\Delta H_{NI}(L_p)$ we seek first the temperature $T^*_{eq}(L_p)$, at which the maxima of the energy distribution $P_{T^*_{eq}}(U^*)$ are of equal height. This temperature turned out to be very close to the susceptibility peak position $T^*_{2,NI}(L_p)$ for all $L_p$. It is known that the energy distribution of a system close to the first order transition

can be approximated reasonably well by a double Gaussian [33]. However, we have obtained better fitting by using a double non-Gaussian distribution of the form:

$$P_{T^*_{eq}}(U^*) \approx c_n \exp\left[-\frac{(U^*-U^*_{nem})^2}{\alpha_{nem}} - \frac{(U^*-U^*_{nem})^3}{\beta_{nem}} - \frac{(U^*-U^*_{nem})^4}{\gamma_{nem}}\right]$$

$$+ c_i \exp\left[-\frac{(U^*-U^*_{iso})^2}{\alpha_{iso}} - \frac{(U^*-U^*_{iso})^3}{\beta_{iso}} - \frac{(U^*-U^*_{iso})^4}{\gamma_{iso}}\right], \quad (7)$$

where the expected values $U_{nem}$ and $U_{iso}$ and the fitting coefficients are obtained numerically, by using the least-squares method. The dimensionless latent heat per particle was then estimated at $T^*_{eq}(L_p)$ as $\Delta H^*_{NI}(L_p) = U^*_{iso} - U^*_{nem}$ (see, Fig. 3). To get a better accuracy, we have used the following average:

$$\langle \Delta H^*_{NI}(L_p) \rangle_{\pm} = \frac{1}{3}(\Delta H^*_{NI}(L_p) + \Delta H^*_{NI+}(L_p) + \Delta H^*_{NI-}(L_p)),$$

where $\Delta H^*_{NI+}(L_p)$ has been estimated similar to $\Delta H^*_{NI}(L_p)$ at $T^*_{eq}(L_p) + \delta T^*$ and $\Delta H^*_{NI-}(L_p)$ has been estimated at $T^*_{eq}(L_p) - \delta T^*$. Here (for the pure model) we choose $\delta T^* = 0.0005$. These estimates $\langle \Delta H^*_{NI}(L_p) \rangle_{\pm}$ do not exhibit a finite-size scaling dependence within the accuracy of our calculations (see, Fig. 4). The latent heat for an infinite system can be derived as the average over all simulated lattice sizes:

$$\Delta H^*_{NI}(\infty_p) = \langle \langle \Delta H^*_{NI}(L_p) \rangle_{\pm} \rangle_{L_p} = 0.179 \pm 0.005. \quad (8)$$

Similar methodology has been used to evaluate the order parameter at the transition $S_{NI}$. In this case the distribution $P_{T^*_{eq}}(U^*)$ is reweighted at $T^*_{2,NI}(L_p)$. The isotropic maximum, that is very low, was fitted by a Gaussian and the nematic maximum by a non-Gaussian:

$$P'_{T^*_{2,NI}}(S) \approx c'_n \exp\left[-\frac{(S-S_{nem})^2}{\alpha'_{nem}} - \frac{(S-S_{nem})^3}{\beta'_{nem}} - \frac{(S-S_{nem})^4}{\gamma'_{nem}}\right]$$

$$+ c'_i \exp\left[-\frac{(S-S_{iso})^2}{\alpha'_{iso}}\right] \quad (9)$$

(see, Fig. 5); moreover, we have assumed $S_{NI}(L_p) = S_{nem}$. Similar to the case of $\Delta H^*_{NI}(L_p)$, the averaging in the form $\langle S_{NI}(L_p) \rangle_{\pm} = \frac{1}{3}(S_{NI}(L_p) + S_{NI+}(L_p) + S_{NI-}(L_p))$ has been used (the + and − signs have the same meanings as above). The values for $\langle S_{NI}(L_p) \rangle_{\pm}$ do not exhibit the $L_p$



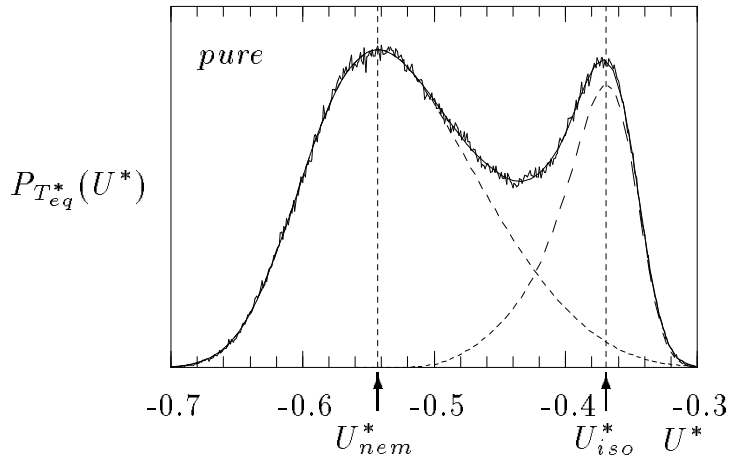


Figure 3. Histogram of the energy distribution (the pure model, $L_p = 24$) at $T^*_{eq}$ and its fit by a double non-Gaussian according to Eq. 7 (the fit practically coincides with the histogram). A nematic and an isotropic non-Gaussian also are shown separately. Their expected values are $U^*_{nem}$ and $U^*_{iso}$, respectively.

dependence within the statistical errors (see, Fig. 6). The average value over all simulated lattice sizes

$$S_{NI}(\infty_p) = \langle \langle S_{NI}(L_p) \rangle_{\pm} \rangle_{L_p} = 0.333 \pm 0.005. \quad (10)$$

is used as an estimate for an infinite system. The results obtained for the latent heat and for the order parameter are more accurate in comparison with our previous study [21], in which a system of single size has been simulated, and in which the FS technique has not been applied to the simulation data.

To conclude this section, the pure model undergoes a well pronounced first order NI transition. This conclusion follows from a finite-size behaviour of the transition temperature, of the heat capacity and susceptibility. The latent heat and the order parameter at the transition are obtained by fitting the corresponding histograms. These properties are of particular interest. We would like to compare them with a weakly diluted case which is the subject of the following section.

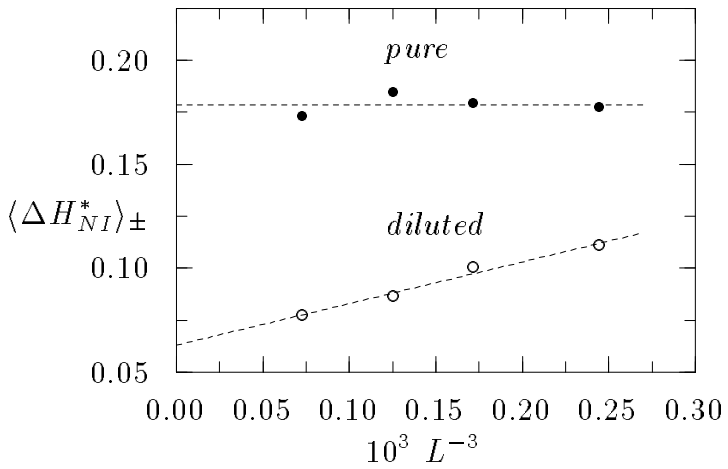


Figure 4. Finite-size scaling behavior of the latent heat of the NI transition calculated as $U^*_{iso} - U^*_{nem}$ and averaged over the vicinity of $T^*_{eq}$. Black circles represent the pure model, the average is shown by the dashed line. Empty circles are for the diluted model, a dashed line corresponds to the linear fit.

## 3. The Nematic-Isotropic Transition in a Weakly Dilute Model

The method described above now is applied to study a weakly dilute model. We have used a so-called random dilution, i.e. when $N_m$ randomly chosen lattice sites are assumed to be occupied by quenched impurities. The other sites, $N_f = N - N_m$, are characterized by the unit vectors $\hat{u}_i$, which describe the orientational interactions between liquid crystal molecules. Similar to the pure model, a nearest neighbours interaction between $\hat{u}_i$ and $\hat{u}_j$ is assumed, also we assume that there is no interaction between the impurities and $\hat{u}_i$. Therefore, only the effects of excluded volume are taken into account. A porous medium formed by impurities may be thought to consists of highly interconnected pores. We consider the case of a weak dilution, $c = N_m/N = 0.05$, which may correspond to a LC confined in a highly porous medium. Due to the CPU time limitations, we have averaged the results over not more than three quenched configurations of impurities for each lattice size.



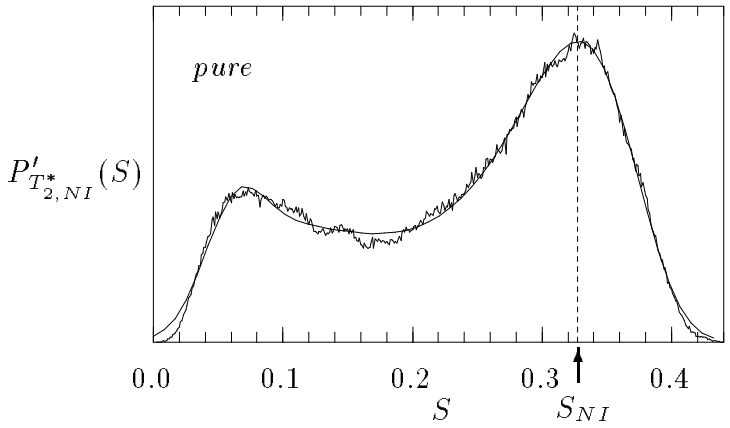


Figure 5. Histogram of the order parameter distribution (the pure model, $L_p = 24$) at the temperature $T^*_{2,NI}$ and its fit by a sum of a Gaussian and a non-Gaussian according to Eq. 9. The expected value of a nematic non-Gaussian gives the order parameter at the transition, $S_{NI}$.

Similar to the pure model, we denote the NI transition temperature of the dilute model of linear size $L_d$ estimated in the framework of a procedure denoted by $m$ by $T^*_{m,NI}(L_d)$. An estimate for the NI transition temperature from the peak for $C^*_v(L_d)$ and for $\chi^*(L_d)$ corresponds to $m = 1, 2$, respectively, and from the minimum of $V_4$ corresponds to $m = 3$. We have observed the shift of the transition temperature of the order $(T^*_{m,NI}(L_p) - T^*_{m,NI}(L_d))/T^*_{m,NI}(L_p) \approx c = 0.05$ for each lattice size in accordance with a mean field estimate. A finite-size scaling behaviour for the first order transition, $T^*_{m,NI}(L_d) - T^*_{m,NI}(\infty_d) \sim L_d^{-3}$, holds very well within the accuracy of our data (see, Fig. 7). For an infinite system, we obtain

$$T^*_{NI}(\infty_d) = 1.0035 \pm 0.0002. \qquad (11)$$

Further confirmation of the first order nature of the transition in the dilute model is the finite size scaling behaviour of the maxima $C^*_{v\,\max}(L_d)$ and $\chi^*_{\max}(L_d)$. The heights of the maxima are essentially supressed, compared with the pure model. But their $L_d^3$ dependence expected for the first order transition is still pronounced (Fig. 8).

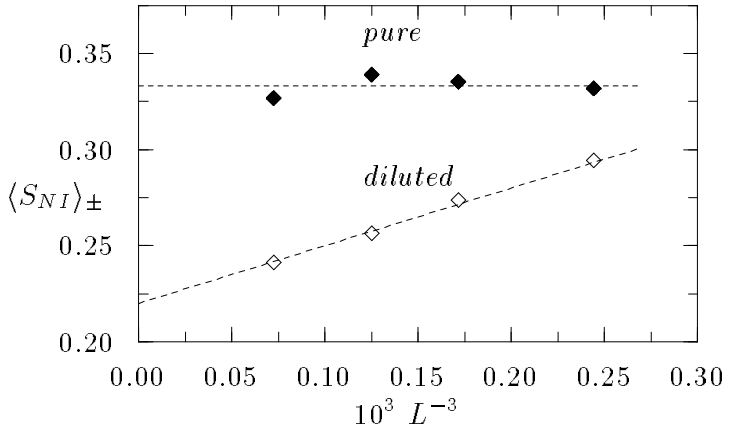


Figure 6. Finite-size scaling behavior of the order parameter at the NI transition obtained from the fits at $T^*_{2,NI}$ and averaged over the vicinity at this temperature. Black diamonds represent the pure model, the average is shown as the dashed line. Empty diamonds are for the diluted model, the dashed line is a linear fit.

The presence of dilution has a strong effect on the form of the energy and order parameter distributions, $P_{T^*}(U^*)$ and $P'_{T^*}(S)$. Even for the largest lattice size simulated, $L = 24$, the double-maxima form for the energy distribution is not observed. This is due to a much weaker first order transition. The distributions for two coexisting phases intersect essentially and it is practically impossible to evaluate the spinodal points for this case. Therefore, we are not able to define formally the temperature $T^*_{eq}$, with equally heighted maxima (as for the pure model). Instead, we have used the temperature where the upper part of the distribution has a symmetric shape (see, Fig. 9). Similar fitting formula for $P_{T^*}(U^*)$ (7) was used to extract the expected values for $U^*_{nem}$ and $U^*_{iso}$, and to estimate a latent heat of the transition $\Delta H^*_{NI}(L_d) = U^*_{iso} - U^*_{nem}$ (see, Fig. 9). We have observed that this procedure is very sensitive to the accuracy of the distribution tails. The accuracy can be unsufficient for the simulated temperature farther from $T^*_{eq}$. In this case, an additional curvature of the distribution tails is present, and the least-squares method fails to fit the histograms correctly. Similar to the pure case, we have



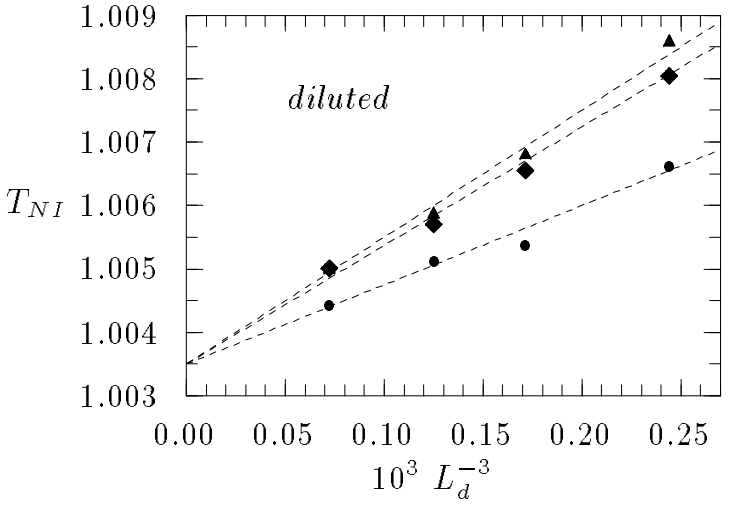


Figure 7. Finite-size scaling behavior of the NI transition temperature in the diluted model defined by different ways (the meaning of the symbols is the same as in Fig. 1), $L_d$ is the linear size of the simulated system.

calculated the average $\langle \Delta H^*_{NI}(L_d)\rangle_{\pm} = \frac{1}{3}(\Delta H^*_{NI}(L_d) + \Delta H^*_{NI+}(L_d) + \Delta H^*_{NI-}(L_d))$ for each $L_d$, where $\Delta H^*_{NI+}(L_d)$ has been estimated at $T^*_{eq}(L_d) + \delta T^*$ and correspondingly the value for $\Delta H^*_{NI-}(L_d)$ at temperature $T^*_{eq}(L_d) - \delta T^*$. The shift of the temperature, $\delta T^* = 0.00025$, was chosen twice smaller, in comparison with the pure model. At these shifted temperatures, $T^*_{eq}(L_d) \pm \delta T^*$, the distribution is essentially asymmetric with the isotropic or nematic maxima clearly seen. Therefore a value, $\Delta H^+(L_d) = U^*_{iso}(T^*_{eq} + \delta T^*) - U^*_{nem}(T^*_{eq} - \delta T^*)$, provides a reasonable upper limit of the latent heat. In the majority of cases it is about 10% higher than the value $\langle \Delta H^*_{NI}(L_d)\rangle_{\pm}$. We have used this fact as an additional test. As one can see in Fig. 4, the values for $\langle \Delta H^*_{NI}(L_d)\rangle_{\pm}$ reflect the $L_d$ dependence. For an infinite system we then obtain the value,

$$\Delta H^*_{NI}(\infty_d) = 0.063 \pm 0.002, \qquad (12)$$

which is essentially lower, if compared with 0.179 for the pure model (8).

The order parameter at the transition is estimated quite similar to the pure model. The only difference is that at $T^*_{2,NI}(L_p) + \delta T^*$, the nematic

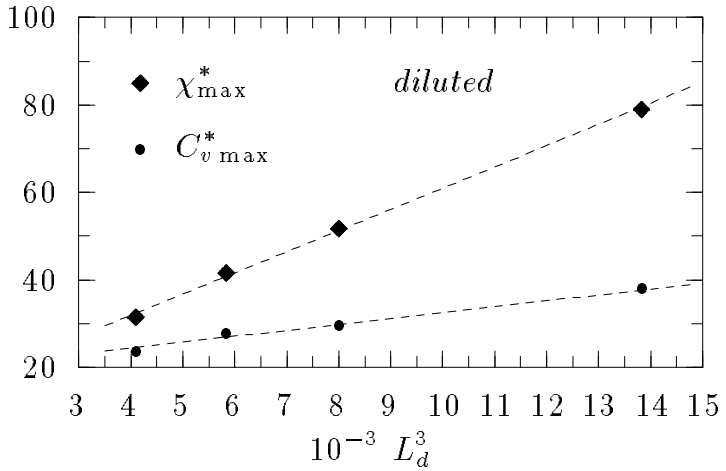


Figure 8. Finite-size scaling behavior of the heat capacity, $C^*_{v\,\max}$, and the susceptibility, $\chi^*_{\max}$, maxima in the vicinity of the NI transition in the diluted model of linear size $L_d$.

maximum for the order parameter is not very well defined to provide fitting successfully. Thus, instead of evaluating the average, $\langle S_{NI}(L_d)\rangle_{\pm}$, we have investigated the dependence of $S_{NI-}(L_d)$ (obtained from the fitting at temperature, $T^*_{2,NI}(L_d) - \delta T^*$, slightly lower than $T^*_{2,NI}(L_d)$) with increasing $\delta T^*$. One might expect linear dependence on $\delta T^*$, if it is chosen small. This is indeed the case for $\delta T^* \in [0.00025, 0.00075]$. We have used this fact as an additional test of stability of the fit at $T^*_{2,NI}(L_d)$. One can note a well pronounced $L_d$ dependence of $S_{NI}(L_d)$ (see, Fig. 6), in contrast to the pure model. Thus, the fitting procedure yields for an infinite system the value,

$$S_{NI}(\infty_d) = 0.220 \pm 0.005. \qquad (13)$$

This value must be compared with the value 0.333 for the pure model (10).

The essential finite-size dependence of the latent heat and of the order parameter for the diluted model can be explained according to the following arguments. The finite-size behaviour of the pure system is governed by the fact that the correlation lenght $\xi$ cannot overcome linear



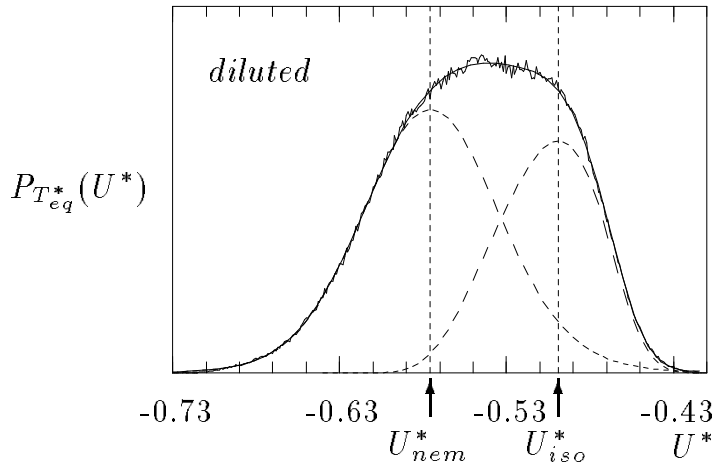


Figure 9. Histogram of the energy distribution (the diluted model, $L_d = 24$) at $T^*_{eq}$ and its fit by a double non-Gaussian according to Eq. 7. A nematic and an isotropic non-Gaussian also are shown separately. Their expected values are $U^*_{nem}$ and $U^*_{iso}$, respectively.

size of the system, $L$. Therefore, in the pure model, all the singularities are scaled by the single characterictic length $\xi$ [30]. In the dilute model, another characteristic length appears, which is an average distance between impurities. Alternatively, influence of the dilution on the phase transition can be described by the parameter $\kappa = c\xi^3$ (proposed by Imry and Wortis [34]), $\kappa$ represents the average number of impurities in a coherence volume. Actually, this parameter measures the relative influence of impurities on the phase transition. We suppose that this parameter must be kept constant for different $L$, rather than the absolute concentration of impurities $c$. For $L < \xi_{bulk}$, one can assume that $\xi_L \approx L$, therefore it seems reasonable to keep constant the parameter $\kappa = cL^3$ for different $L$. Thus, in this case, one must rescale $c$ by $L^{-3}$ with increasing $L$. For $L$ larger than $\xi_{bulk}$, a concentration corresponding to saturation, $c_{bulk}$, would arise. This concentration characterizes a diluted system of infinite size. In the case of a constant dilution, used most generally, one would obtain a progressive suppression of the transition by impurities as $L$ increases (this behavior can be seen from Figs. 4 and 6).

To summarize the results about the influence of a constant, weak, 5% dilution on the NI transition in the lattice model of this study we would like to mention the following. At chosen concentration of impurities, the transition remains the first order transition. However it is much weaker than for the pure case, i.e. in the absence of impurities. A shift of the transition temperature in an infinite system according to Eqs. 6 and 11 can be written in the form of a ratio:

$$\frac{T^*_{NI}(\infty_d)}{T^*_{NI}(\infty_p)} = 0.952 \pm 0.0004. \qquad (14)$$

The supression of the maxima of the heat capacity and of the susceptibility in an infinite system can be obtained from a fit using finite-size data (see, Fig. 10). We have obtained the following ratios:

$$\frac{C^*_{v\,\max}(\infty_d)}{C^*_{v\,\max}(\infty_p)} = 0.35 \pm 0.01, \quad \frac{\chi^*_{\max}(\infty_d)}{\chi^*_{\max}(\infty_d)} = 0.45 \pm 0.01. \qquad (15)$$

A decrease of the latent heat and of the order parameter at the transition point in an infinite system are obtained by using the following values (8,10,12,13). Then, our estimates are,

$$\frac{\Delta H^*_{NI}(\infty_d)}{\Delta H^*_{NI}(\infty_p)} = 0.35 \pm 0.02, \quad \frac{S_{NI}(\infty_d)}{S_{NI}(\infty_p)} = 0.66 \pm 0.02. \qquad (16)$$

It must be mentioned that the effects of lowering the transition temperature, and of suppression of the heat capacity maxima, have been observed previously for: a dilute model of trimers undergoing orientational transition [12], for $q = 3, 4$ state dilute Potts models [13] and for the model of random anisotropy [15]. However, in the present study we have simulated a quite different model and studied the influence of dilution on the susceptibility, on the latent heat and on the order parameter.

## 4. A Comparison with the Experimental Results.

The influence of dilution on thermodynamic properties close to the NI transition can be related to the experimental results for LCs confined in a highly porous media. In particular, Wu *et al.* [9] have studied the NI transition in 8CB LC confined to silica aerogels at different porosity. For $\rho = 0.08$ g cm$^{-3}$ aerogel density (which corresponds roughly to the 5% volume fraction of impurities for our model) the shift of $T_{NI}$ of the magnitude -0.45° has been observed, thus yielding $T^{gel}_{NI}/T^{pure}_{NI} = 0.9986$. The shift, following from our simulations, and given by the ratio (14)



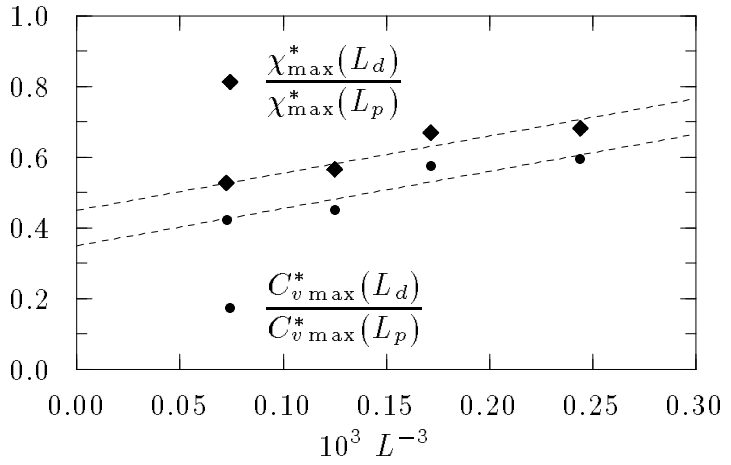


Figure 10. Suppress of the heat capacity, $C^*_{v\,\max}$, and the susceptibility, $\chi^*_{\max}$, maxima resulting from a dilution of the model. Here $L_p = L_d = L$ and indices $d$ and $p$ denote the pure and diluted model, respectively.

is much more pronounced. The integrated enthalpy estimated from the experiment is given by $\delta H = \Delta H + \delta W$, where $\Delta H$ is the latent heat and $\delta W$ is the contribution from the integrated area of a pretransitional region. For the pure model, it follows that $\delta H_{pure} = \Delta H_{pure} + \delta W = (2.1 + 5.58)$ J g$^{-1}$ [9].

It was observed experimentally, that the heat capacity points (plotted versus temperature) for aerogels at different density may be fitted by the same curve in the "pretransitional" region (except the area of about 1.5° width near the transition point) [9]. This lead to the assumption that the density of a confining aerogel influences mostly the value for $\Delta H$, but do not affect strongly the values for $\delta W$. In this case, one can use the ratio $\Delta H_{dil}/\Delta H_{pur} = 0.35$ (16) from the simulations and obtain an estimate, $\delta H_{dil} = \Delta H_{dil} + \delta W = (0.735 + 5.58)$ J g$^{-1}$ = 6.315 J g$^{-1}$. This value is indeed very close to the experimental one, $\delta H_{gel} = 6.28$ J g$^{-1}$, for $\rho = 0.08$ g cm$^{-3}$ aerogel [9]. We can also compare the suppression of the heat capacity maxima by increasing progressively the aerogel density $\rho$. As it follows from the experiment [9], the excess heat capacity $\Delta C_{p\,\max}$ decreases almost linearly with the increasing $\rho$, at $\rho < 0.36$ g cm$^{-3}$.

For the aerogel densities, $\rho_1 = 0.08$ g cm$^{-3}$ and $\rho_2 = 0.17$ g cm$^{-3}$, we then obtain the ratio $\Delta C_{p\,\max}(\rho_2)/\Delta C_{p\,\max}(\rho_1)$ =0.51, which is higher, but nevertheless comparable with the ratio 0.35 (15) obtained in the simulations.

Other experiments for the NI transition in 8CB LC confined to porous glasses have been performed by Iannacchione *et al.* [8]. In the case of a macroporous confinement (1000Å mean pore size), the shift of the transition temperature of -2.05° has been observed. This gives a ratio $T_{NI}^{glass}/T_{NI}^{pure} = 0.993$ which again is higher than the ratio (14). The latent heat $\Delta H_{glass}$ has been shown to decrease and the ratio $\Delta H_{glass}/\Delta H_{pur}$ is 0.74; it is approximately twice larger than (16). Similar discrepancy can be observed for the suppression of the heat capacity, $\Delta C_{p\,\max}(glass)/\Delta C_{p\,\max}(pure) = 0.65$, which is again higher than 0.35 (15). In this context, it is interesting to note, that the values obtained for the smallest lattice, $L_d = 16$, are much closer to the experimental data, giving $\Delta H^*_{NI}(16_d)/\Delta H^*_{NI}(16_p) = 0.63$ and $C^*_{v\,\max}(16_d)/C^*_{v\,\max}(16_p) = 0.60$. Augmenting discrepancy with increasing system size is due to the hypothesis that the dilution concentration, $c$, must be rescaled for a finite size system, keeping the value $c\xi^3$ constant.

We have obtained an essential overestimate for the suppression of the NI transition at a weak 5% dilution, when compared with the experiments. However, our results have been obtained in an infinite volume limit via finite-size scaling. Following the considerations of Imry and Wortis [34], we had supposed that the value $c\xi^3$ must be kept constant at increasing $L$, rather than the impurity concentration $c$. Nevertheless, a shift of the transition temperature is overestimated. Possible explanation of these trends is that one particle in a lattice model describes a group of real molecules, rather than a single one (a simple estimate of Bellini *et al.* [16] has shown that a group of about ten molecules corresponds to a site in the case LL model). Thus, a dilution due to only one site would destroy 6 bonds on the sc lattice, and the energy of 6 surrounding particles (6 groups of molecules) would be essentially underestimated. The temperature of the transition, in fact, is proportional to the number of "surviving" bonds, so it would shift too much. According to that argument, we would like to mention, in particular, that a 5% dilution corresponds effectively to a higher density aerogel, than $\rho = 0.08$ g cm$^{-3}$ implied in a comparison performed above.



## 5. Conclusions

We have performed an extensive Monte Carlo simulations of a weakly dilute liquid crystal lattice model with quenched impurities. The nearest-neighbors interact via the angular part of the Berne-Pechukas potential. The elongation parameter is chosen equal to 3; the corresponding pure system undergoes a well pronounced first order nematic-isotropic transition. The model, in the presence of impurities at constant dilution of 5% has been simulated; four lattice sizes with linear dimensions $L = 16, 18, 20, 24$ have been used. The results of simulations have been averaged over three quenched configurations of impurities for each lattice size. The Ferrenberg-Swendsen reweighting technique has been used in the vicinity of the transition, also a finite-size scaling analysis was applied to the simulation data. The latent heat of the transition and the order parameter have been evaluated by fitting the correspondent histograms by a double non-Gaussian distribution.

We have observed an essential suppression of the nematic-isotropic transition in the model at 5% dilution. This result is in agreement with general theoretical estimates of the influence of the quenched disorder on the first-order transitions [35,36]. However, at a 5% dilution considered here, the nematic-isotropic transition remains an extremely weak first order. A shift of the transition temperature, a suppression of the latent heat and of the heat capacity maxima in the infinite volume limit have been obtained. However, these effects are essentially overestimated, in comparison with the experiments on the 8CB liquid crystal confined to a highly porous media. This behavior seems to appear due to the assumption of rescaled concentration of dilutions for a finite system at a fixed value for the parameter $c\xi^3$.

## 6. Acknowledgments

This work has been supported in parts by the State Fund for Fundamental Investigations under the program DKNT 2.4/173 of the Ukrainian State Commitee for Science and Technology, by the National Committee for Science and Technology (CONACyT) of Mexico under Grant. No.25301-E, and by the National University of Mexico (project DGAPA-IN 111597). One of us (J. I.) is indebted to G. Luckhurst, S. Romano, C. Zannoni and M. P. Allen for very stimulating discussions during the NATO ASI "Advances in the computer simulation of liquid crystals", Erice, 1998.

## References


1. *Liquid Crystals in Complex Geometries Formed by Polymer and Porous Networks*, edited by G. P. Crawford and S. Žumer (Taylor and Francis, 1996).
2. B. Jérôme, Rep. Prog. Phys. **54**, 391 (1991).
3. G. S. Iannacchione and D. Finotello, Phys. Rev. Lett. **69**, 2094 (1992).
4. G. P. Crawford and J. W. Doane, Cond. Matt. News **1**, 5 (1992).
5. M. D. Dadmun and M. Muthukumar, J. Chem. Phys. **98**, 4850 (1993).
6. T. Bellini, N. A. Clark, C. D. Muzny, L. Wu, C. W. Garland, D. W. Schaefer, and B. J. Oliver, Phys. Rev. Lett. **69**, 788 (1992).
7. G. S. Iannacchione, G. P. Crawford, S. Qian, J. W. Doane, D. Finotello, and S. Žumer, Phys. Rev. E **53**, 2402 (1996).
8. G. S. Iannacchione, S. Qian, D. Finotello, and F. M. Aliev, Phys. Rev. E **56**, 554 (1997).
9. L. Wu, B. Zhou, C. W. Garland, T. Bellini, and D. W. Schaefer, Phys. Rev. E **51**, 2157 (1995).
10. M. J. P. Gingras (unpublished).
11. A. Maritan, M. Cieplak, T. Bellini, and J. R. Banavar, Phys. Rev. Lett. **72**, 4113 (1994).
12. M. D. Dadmun and M. Muthukumar, J. Chem. Phys. **97**, 578 (1992).
13. K. Uzelac, A. Hasmy, and R. Jullien, Phys. Rev. Lett. **74**, 422 (1995).
14. A. Maritan, M. Cieplak, and R. Banavar, in *Liquid Crystals in Complex Geometries Formed by Polymer and Porous Networks*, edited by G. P. Crawford and S. Žumer (Taylor and Francis, 1996), p. 483.
15. D. J. Cleaver, S. Kralj, T. J. Sluckin, and M. P. Allen, in *Liquid Crystals in Complex Geometries Formed by Polymer and Porous Networks*, edited by G. P. Crawford and S. Žumer (Taylor and Francis, 1996), p. 467.
16. T. Bellini, C. Chiccoli, P. Pasini, and C. Zannoni, Phys. Rev. E **54**, 2647 (1996).
17. A. M. Ferrenberg and R. H. Swendsen, Phys. Rev. Lett. **61**, 2635 (1988).
18. R. Hashim, G. R. Luckhurst, and S. Romano, Liq. Cryst. **1**, 133 (1986).
19. B. J. Berne and P. Pechukas, J. Chem. Phys. **56**, 4213 (1972).
20. J. Gay and B. J. Berne, J. Chem. Phys. **69**, 3316 (1981).
21. Ja. M. Ilnytskyi, Journ. of Phys. Stud. **1**, 232 (1997); Mol. Cryst. Liq. Cryst. (to be published).





22. P. A. Lebwohl and G. Lasher, Phys. Rev. A **6**, 426 (1972).
23. C. Chiccoli, P. Pasini, F. Biscarini, and C. Zannoni, Molec. Phys. **65**, 1505 (1988).
24. G. I. Fuller, G. R. Luckhurst, and C. Zannoni, Chem. Phys. 92, **105** (1985).
25. S. Romano, Liq. Cryst. **16**, 1015 (1994).
26. S. Romano, Int. J. Mod. Phys. B **9**, 85 (1995)
27. R. Eppenga and D. Frenkel, Mol. Phys. **52**, 1303 (1984).
28. J. Vieillard-Baron, Mol. Phys. **28**, 809 (1974).
29. K. Binder, Z. Phys. B **43**, 119 (1981).
30. K. Binder, Rep. Prog. Phys. **50**, 783 (1987).
31. Zh. Zhang, O. G. Mouritsen, and M. J. Zuckermann, Phys. Rev. Lett. **69**, 2803 (1992).
32. D. J. Cleaver and M. P. Allen, Mol. Phys. **80**, 253 (1993).
33. M. S. S. Challa, D. P. Landau, and K. Binder, Phys. Rev. B **34**, 1841 (1986).
34. Y. Imry and M. Wortis, Phys. Rev. B **19**, 3580 (1979).
35. A. N. Berker, Bull. Am. Phys. Soc. **14**, 1990 (1990).
36. J. Cardy, in *Book of abstracts of the XXth IUPAP International Conference on Statistical Physics*, Paris, 1998, edited by A. Gervois, M. Gingold, and D. Iagolnitzer (UNESCO, Sorbonne, 1998), T1680: IL04/4.

Препринти Інституту фізики конденсованих систем НАН України розповсюджуються серед наукових та інформаційних установ. Вони також доступні по електронній комп'ютерній мережі на WWW-сервері інституту за адресою http://www.icmp.lviv.ua/

The preprints of the Institute for Condensed Matter Physics of the National Academy of Sciences of Ukraine are distributed to scientific and informational institutions. They also are available by computer network from Institute's WWW server (http://www.icmp.lviv.ua/)

Ярослав Миколайович Ільницький
Стефан Соколовскі
Орест Олександрович Пізіо

Фазовий перехід нематик-ізотропна рідина в гратковій моделі з замороженими домішками. Комп'ютерна симуляція за допомогою методу Монте Карло

Роботу отримано 20 листопада 1998 р.

Затверджено до друку Вченою радою ІФКС НАН України

Рекомендовано до друку семінаром відділу статистичної теорії конденсованих систем

Виготовлено при ІФКС НАН України
© Усі права застережені